Observation of enhanced two-photon absorption in ZnS quantum dots at an ultraviolet wavelength

P. Kumbhakar[1*], M. Chattopadhyay[1], R. Sarkar[1], and U. Chatterjee[2]

[1] *Nanoscience Laboratory, Department of Physics, National Institute of Technology, Durgapur, 713209, India*

[2] *Laser Laboratory, Department of Physics, Burdwan University, Burdwan, 713104, India*

[*] *Corresponding author: kumbhakarp@yahoo.com; pathik.kumbhakar@phy.nitdgp.ac.in*

Received February 23, 2011; accepted May 9, 2011; posted online July 29, 2011

Two-photon absorption (2PA) in zinc sulphide (ZnS) and Mn^{2+}-doped ZnS quantum dots is reported by the z-scan technique, with nanosecond pulsed laser radiation at 355 nm. The observed values of the 2PA cross section of all the samples are 10^5 times larger than that of bulk ZnS.

OCIS codes: 190.0190, 160.4236, 190.4180.

doi: 10.3788/COL201109.101902.

Researchers have recently expanded their research interests to find highly potential multiphoton active materials[1−10]. Amongst others, zinc sulphide (ZnS) and Mn^{2+}-doped ZnS (ZnS:Mn) quantum dots (QDs) have been found to be potential materials because of their visible luminescence and interesting nonlinear optical (NLO) properties[5−8,10−12]. Reports on the multiphoton absorption properties of ZnS QDs have been published previously. For example, two-photon absorption (2PA) has been reported by Zheng *et al.* with picosecond laser radiation at 532 nm in 0.5% Mn^{2+}-doped ZnS QDs[7]. Some enhancements in 2PA have been reported in ZnSe/ZnS core/shell at 806 nm and in ZnS quantum structures at 532-nm laser pulses[13,14]. However, to date, there has been no report on the measurement of NLO properties of ZnS and ZnS:Mn QDs in the ultraviolet (UV) region. In this letter, we present our observation of 2PA in undoped ZnS and ZnS:Mn QDs at an UV wavelength of 355 nm. The obtained values of the 2PA cross section in the studied samples are $\sim 10^5$ times larger than that of the available reported value of bulk ZnS[11].

The samples used in this work are freshly prepared through the chemical precipitation method[11]. The synthesized undoped ZnS and 1% and 2.5% Mn^{2+}-doped ZnS samples are henceforth denoted as R_I, R_{II}, and R_{III}, respectively, unless otherwise specified. The UV-visible absorption characteristics of the samples, as obtained from the measurement in a spectrophotometer (Hitachi U-3010), are shown in Fig. 1. An X-ray diffraction measurement of the samples ensures the average particle size (radius) to be ∼1.5 nm[10].

The experimental z-scan set-up used for the measurement of NLO properties is a standard one[2,8,15]. However, in the present experiment, the excitation source of 355-nm radiation is obtained through a third harmonic generation from a Q-switched Nd:YAG laser (10 ns, 10 Hz repetition rate). To avoid the absorption of the input beam in the lens material itself, a quartz lens with a focal length of 7.5 cm is used to focus the 355-nm radiation. The beam waist (w_0) and the confocal parameter (z_0) at the focus are 7 and 350 μm, respectively. After they are dispersed in methanol, the as-synthesized nanopowders are kept in a quartz cuvette with a path length (L) of 2 mm for the z-scan measurement, satisfying the thick sample condition ($L > n_0 z_0$) in the present experiment. Here, n_0 is the linear refractive index of the samples at a 355-nm wavelength. In Fig. 1, the values of the linear absorption coefficient (α) of R_I, R_{II}, and R_{III} samples are 0.50, 0.33, and 0.47 cm^{-1}, respectively, at the excitation wavelength of 355 nm.

In the present experiment, the medium length is larger than the confocal parameter. Therefore, nonlinear refraction (NLR) should be considered in such type of thick medium, i.e., when a Gaussian beam is allowed to pass through the sample. According to the distributed lens model, the on-axis normalized open aperture (OA) transmittance (T_{OA}) can be written as[14]

$$T_{OA} = \{1 + 0.5C_0[\tan^{-1}(p+l) - \tan^{-1}(p)]\}^{-1}, \quad (1)$$

where $p = z/n_0 z_0$, $l = L/n_0 z_0$, $C_0 = q_0\{1 + \tanh(l/2) \times [(3q_0/10) + (q_0^2/8)]\}$, $q_0 = \beta_{2PA} I_0 n_0 z_0$, and $q_0 = 2\pi\gamma n_0 z_0/\lambda$. Here, I_0, β_{2PA}, and γ are the on-axis peak irradiance at focus in W/cm^2, the 2PA coefficient, and the NLR coefficient of the sample, respectively, and λ is the wavelength of the radiation used.

Figure 2 shows our experimental and theoretically fitted OA z-scan transmission traces of all the samples measured at the maximum input beam intensity of 27.4 GW/cm^2. Here, the symbols are the experimental points,

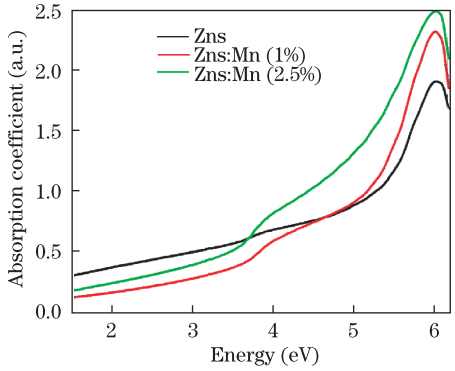

Fig. 1. UV-visible absorption characteristics of undoped ZnS and ZnS:Mn QDs dispersed in methanol.

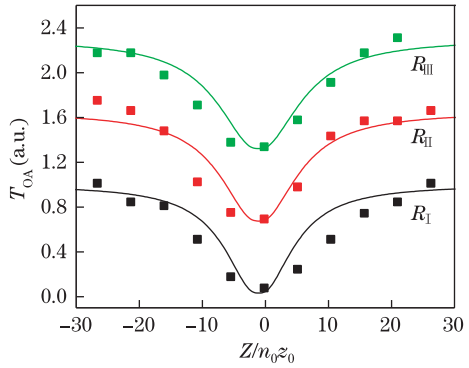

Fig. 2. Normalized transmittance curves of the OA z-scan at 355-nm incident laser radiation for R_I, R_{II}, and R_{III} samples at the peak intensity of 27.4 GW/cm^2. Symbols are the experimental points. The solid curves of all samples are the theoretically fitted ones with the 2PA process in thick media. While drawing the graphs, the baselines are shifted upward to avoid overlapping.

and the solid curves are the theoretically fitted ones using Eq. 1. In Fig. 2, the theoretical curves obtained considering the 2PA clearly show excellent fitting to the experimental data. The observed NLO properties are attributed only to the semiconductor QDs samples, as the quartz cuvette filled with methanol does not show any NLO property. The obtained values of nonlinear absorption (NLA) and NLR coefficients are summarized in Table 1.

The value of the intrinsic 2PA coefficient (β_{2PA}^{Int}) of the samples is deduced using the relation $\beta_{2PA}^{Int} = [\beta_{2PA}(n_0^{soln})^2]/[(n_0^{QDs})^2 f(\pounds)^4]$, where f is the volume fraction of the QDs solutions, and $\pounds$ is the local field correction, which depends on the dielectric constant of the solvent and QDs[12]. The refractive index n_0^{QDs} of the QDs of radius R can be obtained using the relation $^9n_0^{QDs} = \sqrt{1+\frac{n^2-1}{1+(0.375/R)^{1.2}}}$. The wavelength-dependent refractive index (n) of the bulk ZnS is calculated using the Sellmeier dispersion relation[16]:

$$n^2 = 4.4175 + 1.7396\lambda^2/(\lambda^2 - 0.07166). \quad (2)$$

Using the relation $\sigma_2 = \hbar\omega\beta_{2PA}/N_0$ and $N_0 = 6.2\times10^{17}$/cm^3, the 2PA cross section (σ_2) of all samples is calculated. The experimentally obtained values of β_{2PA}^{Int}, σ_2, etc. for all the samples obtained in this work, along with the literature data for bulk ZnS and ZnS QDs, are summarized in Table 1. The obtained values of σ_2 of all samples are $\sim 10^7$ times larger than that of bulk ZnS, and they are at least one order of magnitude larger than those of ZnSe/ZnS core/shell and ZnSe QDs[12]. In Table 1, the calculated values of the NLR coefficient (n_2) of all samples are almost the same and of the same order of magnitude as that of bulk ZnS.

As the values of the incident photon energy (E_p) and the bandgap energy (E_g) of the sample are ~3.5 and ~5.16 eV, respectively; the condition $2E_p > E_g$ is satisfied in all samples. This finding clearly confirms the dominance of 2PA in the present experiment[3]. In another calculation, using the dispersion scaling rule given by Sheik-Bahae *et al.*, the normalized 2PA maxima (peak) near the wavelength of 355 nm is obtained by taking the bandgap of the material of 5.2 eV (Fig. 3(a))[15]. In Fig. 3(a), the curves correspond to the normalized 2PA coefficients with different semiconductor bandgap energy values of 3.6, 4, 4.5, 5.2, 5.5, and 6 eV, respectively. At $E_g = 5.2$ eV, the curve shows that the maximum (peak) of the normalized 2PA appears near 355 nm. Conversely, the other curves (i.e., for different bandgaps) show that the position of the maxima (peak) deviates from 355 nm, indicating the higher probability of occurrence of 2PA at 355 nm at the bandgap energy $E_g = 5.2$ eV. Thus, the suitable choice of the bandgap of the semiconductor and that of the corresponding wavelength is the best combination for obtaining a large 2PA.

OA z-scan transmittance traces are also collected at four different values of the input intensities for the R_I sample. All the experimental data are theoretically fitted as described above. Based on the theoretical fitting, the intensity dependent values of β_{2PA}^{Int} are calculated, as shown in Fig. 3(b). In the same figure, the solid curve is obtained by a second-order polynomial fitting of the experimental data (symbols) to show only the trends of variation of the experimental data. In Fig. 3(b), with the increasing intensity I_0, the 2PA coefficients initially increase and then decrease with increasing I_0. The observed variation of the NLA coefficient with the intensity demonstrates the presence of two-photon-generated free-carrier nonlinearities resulting in the effective fifth-order nonlinearity under strong excitation[7,17–19]. The value of the free-carrier absorption (FCA) cross section induced by the 2PA in the R_{II} sample is calculated from the measured intensity-dependent OA z-scan traces using the fast analytical procedure of Gu

Table 1. 2PA Coefficients, 2PA Cross Sections, and NLR Coefficients of All Samples Measured at 355 nm Wavelength at 27.4-GW/cm^2 Intensity

Sample	β^{Int} (cm/GW)		σ_2(GM)		γ ($\times10^{-14}$cm^2/W)	n_2 ($\times10^{-12}$ e.s.u)	
	This Work	Lit. Data	This Work	Bulk	This Work	This Work	Bulk
R_I	3.8×10^5	1[a], 1.18[b], 1±0.3[c]	2.12×10^5	5.14×10^{-2}[d]	1.46	8.4	3.3[a]
R_{II}	4.4×10^5		2.47×10^5		1.47	8.6	
R_{III}	5.7×10^5		3.20×10^5		1.50	8.7	

[a]Bulk ZnS at 610 nm[11], [b]ZnS QDs at 532 nm[7], [c]ZnS QDs at 795 nm[12], and [d]Bulk ZnS at 532 nm[13]

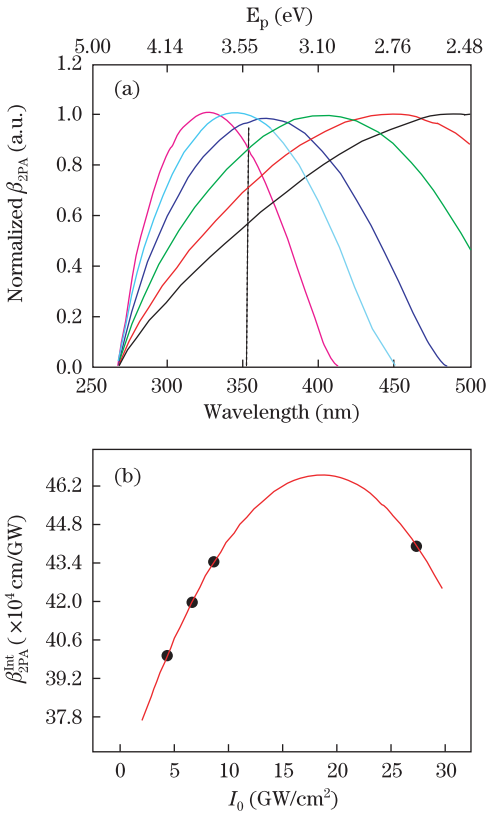

Fig. 3. (a) Wavelength dispersion of normalized 2PA coefficients for bulk semiconductor considering the 2PA scaling rule, as reported by Sheik-Bahae *et al.*[15]. Top axis shows the values of the energy (E_p) corresponding to each wavelength of the x axis; (b) variation of the 2PA coefficient (β_{2PA}^{Int}) with the irradiance at the focus (I_0).

et *al.*[18]. From the measured OA z-scan traces, we calculate the value of additional absorbance ($\Delta\alpha$) for higher values of the incident peak irradiances (I_0). This plot is shown in Fig. 4, where the symbols denote the experimental points, and the solid curve is drawn using

$$\frac{\Delta\alpha}{I_0} = 2.71 - 0.074 I_0. \quad (3)$$

Equation (3) is obtained by the least square fitting of the experimental data. From Eq. (3), the value of the NLA coefficient caused by pure 2PA is β_{2PA} = 2.71 cm/GW, which corresponds to β_{2PA}^{int}=3.9×10^5 cm/GW. By following the analytical procedure elaborated in Ref. [18], the slope (s) of the fitted straight line is related to the FCA cross section (σ_a) of the sample by the following relation[18]:

$$\sigma_a = -\frac{1.36 s E_p \times 10^{-9}}{\tau_e}\sqrt{\frac{1+0.59\,(\tau/\tau_e)^{\sqrt{3}}}{0.59\,(\tau/\tau_e)^{\sqrt{3}}}}. \quad (4)$$

By substituting E_p=3.5 eV, s = 0.074, the free-carrier lifetime in ZnS(τ_e)=0.8 ns[19], and the duration of the incident laser pulse τ =10 ns in Eq. (4), we obtain σ_a= –0.04×10^{-18} cm^2.

The average particle size of 1.5 nm of the QDs is less than the exciton Bohr radius of 2.2 nm in bulk ZnS. The huge enhancement in the 2PA cross section is attributed

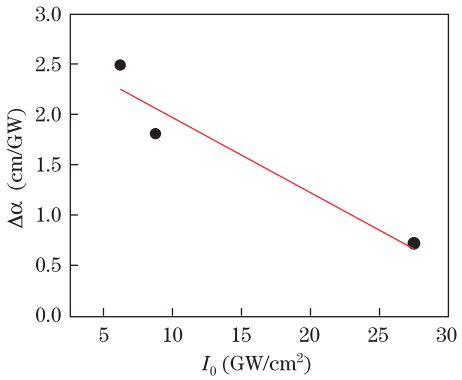

Fig. 4. Variation of the additional absorption ($\Delta\alpha$) with the input irradiance (I_0). The solid curve is obtained by the least square fitting of the experimental data (symbols).

to the quantum confinement effects as well as to the large surface to volume ratio of the QDs. As the size is reduced, the oscillator strength is concentrated into only a few transitions, leading to the enhancement of the nonlinearity of the materials. Moreover, as described above, the use of the 355-nm wavelength in the present experiment also favors the large enhancement in the 2PA coefficient of ZnS QDs. In a QD, the absorption is determined by the confined transitions; however, in the refractive index, a large number of off-resonant but still bulk-like states are contributed[20].

In conclusion, we present here a 10^5 time-enhanced 2PA coefficient both in the ZnS and (1–2.5%) Mn^{2+}-doped ZnS QDs at 355 nm by the z-scan technique. This huge enhancement in the 2PA in the samples is attributed to the quantum confinement effects. The observation of intensity-dependent NLA in a sample is explained by considering the simultaneous presence of 2PA and 2PA-induced FCA in the investigated sample. As the particle size is reduced below the exciton Bohr radius of the material, the oscillator strength is concentrated into only a few transitions, leading to the enhancement of the nonlinearity of the materials. Moreover, the beneficial combination of the experimental parameters, such as the incident photon energy and the bandgap of the used samples, provides the highest probability for achieving 2PA in the investigated samples. The present observation of the enhanced NLA and NLR of the undoped and Mn^{2+}-doped ZnS samples at 355 nm, combined with our previous observations at 532 and 1 064 nm[5,8], shows that these QDs are excellent materials for use in optoelectronic and biophotonic devices.

This work was supported by the DST of the Government of India under Grant No. SR/FTP/PS-67/2008.

References

1. B. Gu, K. Lou, J. Chen, H. T. Wang, and W. Ji, J. Opt. Soc. Am. B **27,** 2438 (2010).
2. E. W. Van Stryland and M. Sheik-Bahae, M. G. Kuzyk and C. W. Dirk (Eds.), *Characterization Techniques and Tabulations for Organic Nonlinear Materials* (Marcel Dekker Inc., 1998).
3. B. Gu, Y. X. Fan, J. Chen, H. T. Wang, J. He, and W. Ji, J. Appl. Phy. **102,** 083101 (2007).
4. A. Penzkofer and Falkenstein, Opt. Commun. **16,** 247 (1976).

5. M. Chattopadhyay, P. Kumbhakar, R. Sarkar, and A. K. Mitra, Appl. Phys. Lett. **95,** 163115 (2009).
6. R. A. Ganeev, J. Opt. A: Pure Appl. Opt. **7,** 717 (2005).
7. J.-J. Zheng, G.-L. Zhang, Y.-X. Guo, X.-Y. Wang, W.-J. Chen, X.-S. Zhang, and Y.-L. Hua, Chin. Phys. Lett. **23,** 3097 (2006).
8. M. Chattopadhyay, P. Kumbhakar, C. S. Tiwary, R. Sarkar, A. K. Mitra, and U. Chatterjee, J. Appl Phys. **105,** 024313 (2009).
9. N. Venkatram, R. Sathyavathi, and D. N. Rao, Opt. Express **15,** 12258 (2007).
10. R. Sarkar, C. S. Tiwary, P. Kumbhakar, S. Basu, and A. K. Mitra, Physica E **40,** 3115 (2008).
11. T. D. Krauss and F. W. Wise, Appl. Phys. Lett. **65,** 1739 (1994).
12. A. D. Lad, P. P. Kiran, D. More, G. R. Kumar, and S. Mahamuni, Appl. Phys. Lett. **92,** 043126 (2008).
13. V. V. Nikesh, A. Dharmadhikari, H. Ono, S. Nozaki, G. R. Kumar, and S. Mahamuni, Appl. Phys. Lett. **84,** 4602 (2004).
14. W. P. Zang, J. G. Tian, Z. B. Liu, W. Y. Zhou, F. Song, and C. P. Zhang, J. Opt. Soc. Am. B. **21,** 63 (2004).
15. M. Sheik-Bahae, D. C. Hutchings, D. J. Hagan, and E. W. Van Stryland, IEEE. J. Quantum Electron. **27,** 1296 (1991).
16. M. Bass, *Handbook of Optics* (second ed.)(McGraw Hill, New York, 1995).
17. A. Knorr, R. Binder, E. M. Wright, and S. W. Koch, Opt. Lett. **18,** 1538 (1993).
18. B. Gu, Y. Sun, and W. Ji, Opt. Express **16,** 17745 (2008).
19. J. Wang, M. Sheik-Bahae, A. A. Said, D. J. Hagan, and E. W. Van Stryland, J. Opt. Soc. Am. B **11,** 1009 (1994).
20. D. J. Hagan, E. W. Van Stryland, M. J. Soileau, Y. Y. Wu, and S. Guha, Opt. Lett. **13,** 315 (1988).